Monte Carlo Solution of a Spatially-Discrete Transport Equation Part I: Transport

Todd J. Urbatsch, Jim E. Morel, and John C. Gulick*
XTM – Transport Methods Group, MS D409
Los Alamos National Laboratory
Los Alamos, New Mexico 87545 (US)
tmonster@lanl.gov jim@lanl.gov gulick@engr.orst.edu

Abstract

We present the S_∞ method, a hybrid neutron transport method in which Monte Carlo particles traverse discrete space. The goal of any deterministic/stochastic hybrid method is to couple selected characteristics from each of the methods in hopes of producing a better method. The S_∞ method has the desirable features of the lumped, linear-discontinuous (LLD) spatial discretization, yet it has no ray-effects because of the continuous angular variable. We derive the S_∞ method for the steady-state, mono-energetic transport equation in one-dimensional slab geometry with isotropic scattering and an isotropic internal source. We demonstrate the viability of the S_∞ method by comparing our results favorably to analytic and deterministic results.

1 Introduction and Motivation

We present a hybrid Monte Carlo method that solves the neutron transport equation continuously in angle, but discretely in space according to the lumped, linear-discontinuous (LLD) spatial discretization scheme. We call this hybrid method the S_∞ method because it corresponds to a deterministic S_N method with an infinite number of discrete directions. An advantage of S_∞ over S_N is that, by not discretizing in angle, we eliminate ray-effects, a deficiency of the S_N method.

We hope to ultimately extend the S_∞ method to nonlinear, thermal radiative transfer problems, where it is not clear that current Monte Carlo thermal radiation methods [Fleck and Cummings, 1971] have the correct diffusion limit. We know that, in the thick equilibrium-diffusion limit, S_∞'s LLD spatial discretization scheme goes over to a convergent and robust differencing of the diffusion equation. The interior solutions may not necessarily be correct when the boundary layers are not resolved, but they are nevertheless well-behaved and fairly accurate [Morel, et al., 1996]. In nonlinear thermal radiative transfer, the material equation is typically solved deterministically regardless of how the radiation equation is solved. Therefore, S_∞ has a potential advantage over regular Monte Carlo, whose ability to converge to the exact solution is negated by the deterministic truncation errors from the material equation. Furthermore, with the LLD scheme's correct diffusion limit in nonlinear radiative transfer, S_∞ may require fewer cells and fewer small-matrix inversions, making it faster than regular, spatially-continuous Monte Carlo.

*Department of Nuclear Engineering, Oregon State University, Corvalis, Oregon 97331 (US).

A more immediate motivation for developing the S_∞ method is our need for a method to which we can compare and couple a related method, which is based on diffusion instead of transport [Urbatsch, et al., 1999].

2 Discretized Transport Equation

We begin with the steady-state neutron transport equation in one-dimensional slab geometry, with no energy dependence, isotropic internal sources, and isotropic scattering,

$$\mu \frac{\partial \psi(x,\mu)}{\partial x} + \sigma_t(x)\psi(x,\mu) = \frac{\sigma_s(x)}{2}\phi(x) + \frac{q(x)}{2} \quad , \tag{1}$$

where μ is the cosine of the polar angle, $x \in [0, X]$ is the spatial variable in cm, X is the slab width, $\psi(x,\mu)$ is the angular flux, $\sigma_t(x)$ is the macroscopic total cross section, $\sigma_s(x)$ is the macroscopic scattering cross section, $q(x)$ is the isotropic internal source, and $\phi(x)$ is the scalar flux,

$$\phi(x) = \int_{-1}^{1} \psi(x,\mu)\, d\mu \quad . \tag{2}$$

The boundary conditions are that the incoming angular fluxes are specified,

$$\psi(0,\mu) = f(\mu) \quad , \quad \mu > 0 \quad , \tag{3}$$

$$\psi(X,\mu) = g(\mu) \quad , \quad \mu < 0 \quad . \tag{4}$$

We spatially discretize the transport equation with the lumped, linear-discontinuous (LLD) discretization scheme [Morel, et al., 1996]. First, the slab is divided into N cells, such that cell i, where $i \in [1, N]$, has edges $x_{i-1/2}$ and $x_{i+1/2}$. The cross sections are assumed constant in each cell. The angular flux, scalar flux, and the source *within* each cell i is assumed linear,

$$\psi(x,\mu) = \psi_i^L(\mu)V_i^L(x) + \psi_i^R(\mu)V_i^R(x) \quad , \tag{5}$$

$$\phi(x) = \phi_i^L V_i^L(x) + \phi_i^R V_i^R(x) \quad , \tag{6}$$

$$q(x) = q_i^L V_i^L(x) + q_i^R(x) V_i^R \quad , \tag{7}$$

where

$$V_i^L(x) = \frac{x_{i+1/2} - x}{\Delta x_i} \quad , \tag{8}$$

$$V_i^R(x) = \frac{x - x_{i-1/2}}{\Delta x_i} \quad , \tag{9}$$

and where Δx_i is the width of cell i,

$$\Delta x_i = x_{i+1/2} - x_{i-1/2} \quad . \tag{10}$$

A cell-average quantity is defined as

$$t_i^A = \frac{1}{2}\left(t_i^L + t_i^R\right) \quad , \tag{11}$$

where t=ψ, ϕ, or q. The angular flux at cell interfaces is defined to be continuous in the direction of travel [Morel, et al., 1996],

$$\psi(x_{i+1/2},\mu) = \begin{cases} \psi_i^R(\mu) & \mu > 0 \\ \psi_{i+1}^L(\mu) & \mu < 0 \end{cases} \quad . \tag{12}$$

Substituting the linear expressions for the angular flux, Eq. (5), the scalar flux, Eq. (6), and the internal source, Eq. (7), into the transport equation, Eq. (1), we have

$$\begin{aligned} &\mu \frac{\partial}{\partial x} \left[\psi_i^L(\mu) V_i^L(x) + \psi_i^R(\mu) V_i^R(x) \right] + \sigma_{t,i} \left[\psi_i^L(\mu) V_i^L(x) + \psi_i^R(\mu) V_i^R(x) \right] \\ &\quad = \frac{\sigma_{s,i}}{2} \left[\phi_i^L(\mu) V_i^L(x) + \phi_i^R(\mu) V_i^R(x) \right] + \frac{1}{2} \left[q_i^L V_i^L(x) + q_i^R V_i^R(x) \right] \quad . \end{aligned} \tag{13}$$

Multiplying Eq. (13) by $V_i^L(x)$, integrating over spatial cell i, and considering the interface conditions in Eq. (12), we obtain two equations for $\psi_i^L(\mu)$, one for $\mu > 0$ and one for $\mu < 0$. Similarly, multiplying Eq. (13) by $V_i^R(x)$, integrating over spatial cell i, and considering the interface conditions, we obtain two equations for $\psi_i^R(\mu)$, one for $\mu > 0$ and one for $\mu < 0$, for a total of four equations. These four equations constitute the linear-discontinuous (LD) discretization scheme. Multiplying through by 2, we present the four equations as two matrix equations, one for $\mu > 0$ and one for $\mu < 0$,

$$\begin{bmatrix} \mu & \mu \\ -\mu & \mu \end{bmatrix} \begin{bmatrix} \psi_i^L(\mu) \\ \psi_i^R(\mu) \end{bmatrix} + \tau_i \mathbf{A} \begin{bmatrix} \psi_i^L(\mu) \\ \psi_i^R(\mu) \end{bmatrix} = \frac{\tau_{s,i}}{2} \mathbf{A} \begin{bmatrix} \phi_i^L(\mu) \\ \phi_i^R(\mu) \end{bmatrix} + \frac{\Delta x_i}{2} \mathbf{A} \begin{bmatrix} q_i^L \\ q_i^R \end{bmatrix} \quad , \quad \mu > 0 \quad , \tag{14}$$

$$\begin{bmatrix} -\mu & \mu \\ -\mu & -\mu \end{bmatrix} \begin{bmatrix} \psi_i^L(\mu) \\ \psi_i^R(\mu) \end{bmatrix} + \tau_i \mathbf{A} \begin{bmatrix} \psi_i^L(\mu) \\ \psi_i^R(\mu) \end{bmatrix} = \frac{\tau_{s,i}}{2} \mathbf{A} \begin{bmatrix} \phi_i^L(\mu) \\ \phi_i^R(\mu) \end{bmatrix} + \frac{\Delta x_i}{2} \mathbf{A} \begin{bmatrix} q_i^L \\ q_i^R \end{bmatrix} \quad , \quad \mu < 0 \quad , \tag{15}$$

where we have substituted expressions for the total and scattering optical thicknesses,

$$\tau_i = \sigma_{t,i} \Delta x_i \quad , \tag{16}$$

$$\tau_{s,i} = \sigma_{s,i} \Delta x_i \quad , \tag{17}$$

and where $\mathbf{A}$ is the linear-discontinuous spatial averaging matrix,

$$\mathbf{A} = \begin{bmatrix} 2/3 & 1/3 \\ 1/3 & 2/3 \end{bmatrix} \quad . \tag{18}$$

Next, we "lump" the spatial averaging matrix $\mathbf{A}$ by moving the off-diagonal element to the diagonal element in a row and summing, resulting in an identity matrix [Morel, et al., 1996],

$$\mathbf{A} = \begin{bmatrix} 2/3 & 1/3 \\ 1/3 & 2/3 \end{bmatrix} \longrightarrow \mathbf{A}_{lumped} = \begin{bmatrix} 1 & 0 \\ 0 & 1 \end{bmatrix} \quad . \tag{19}$$

Substituting $\mathbf{A}_{lumped}$ for $\mathbf{A}$ and expanding the source, we obtain the LLD equations

$$\begin{bmatrix} \tau_i + \mu & \mu \\ -\mu & \tau_i + \mu \end{bmatrix} \begin{bmatrix} \psi_i^L(\mu) \\ \psi_i^R(\mu) \end{bmatrix} = \begin{bmatrix} \frac{1}{2} \tau_{s,i} \phi_i^L + 2\mu \psi_{i-1}^R(\mu) + \frac{1}{2} q_i^L \Delta x_i \\ \frac{1}{2} \tau_{s,i} \phi_i^R + \frac{1}{2} q_i^R \Delta x_i \end{bmatrix} \quad , \quad \mu > 0 \quad , \tag{20}$$

$$\begin{bmatrix} \tau_i - \mu & \mu \\ -\mu & \tau_i - \mu \end{bmatrix} \begin{bmatrix} \psi_i^L(\mu) \\ \psi_i^R(\mu) \end{bmatrix} = \begin{bmatrix} \frac{1}{2} \tau_{s,i} \phi_i^L + \frac{1}{2} q_i^L \Delta x_i \\ \frac{1}{2} \tau_{s,i} \phi_i^R - 2\mu \psi_{i+1}^L(\mu) + \frac{1}{2} q_i^R \Delta x_i \end{bmatrix} \quad , \quad \mu < 0 \quad . \tag{21}$$

The LLD discretization scheme achieves a greater robustness than the LD scheme at the cost of second-order accuracy instead of third-order [Morel, et al., 1996].

3 Balance Equations

The S_∞ method requires a balance equation for each of the discretized transport equations, Eqs. (20) and (21). Summing the rows in Eq. (20) and dividing through by 2, we obtain the following balance equation for positive directions,

$$\mu\psi_i^R + \tau_i\psi_i^A = Q_i^+ = \mu\psi_{i-1}^R(\mu) + \frac{\tau_{s,i}}{2}\phi_i^A + \frac{1}{2}\Delta x_i q_i^A \quad , \quad \mu > 0 \quad , \tag{22}$$

where Q_i^+ is the total source in cell i for $\mu > 0$. Dividing through by Q_i^+, we obtain a probability equation,

$$P_{leak}^+ + P_{collide}^+ = 1 \quad , \quad \mu > 0 \quad , \tag{23}$$

where the probability of leaking out the right side of the cell is

$$P_{leak}^+ = \frac{\mu\psi_i^R}{Q_i^+} \quad , \quad \mu > 0 \quad , \tag{24}$$

and the probability of colliding in the cell is

$$P_{collide}^+ = \frac{\tau_i\psi_i^A}{Q_i^+} \quad , \quad \mu > 0 \quad . \tag{25}$$

Similarly, we sum the rows of Eq. (21) and divide by 2 to get a balance equation for negative directions,

$$-\mu\psi_i^L + \tau_i\psi_i^A = Q_i^- = -\mu\psi_{i+1}^L(\mu) + \frac{1}{2}\tau_{s,i}\phi_i^A + \frac{1}{2}\Delta x_i q_i^A \quad , \quad \mu < 0 \quad , \tag{26}$$

where Q_i^- is the total source in cell i for $\mu < 0$. Dividing through by Q_i^-, we obtain a probability equation,

$$P_{leak}^- + P_{collide}^- = 1 \quad , \quad \mu < 0 \quad , \tag{27}$$

where the probability of leaking out the left side of the cell is

$$P_{leak}^- = \frac{-\mu\psi_i^L}{Q_i^-} \quad , \quad \mu < 0 \quad , \tag{28}$$

and the probability of colliding in the cell is

$$P_{collide}^- = \frac{\tau_i\psi_i^A}{Q_i^-} \quad , \quad \mu < 0 \quad . \tag{29}$$

4 The S_∞ Process

The S_∞ method considers Monte Carlo particles that are continuous in angle and that traverse discrete space. It is similar to regular analog Monte Carlo in most ways, except that particles do not traverse space continuously. Let us step through the process.

4.1 Source

We have three types of sources: incoming flux, internal source, and scattering. The first two types of sources are of the initiating type, whereas the scattering type appears during the particle's life.

Suppose we have an incoming flux on the left side of the slab. We assign the particle a weight, wt, of unity and sample its direction cosine, $\mu > 0$. Next, we solve the appropriate discretized transport equation, Eq. (20), in cell 1, with every element of the source equal to zero except for the incoming current, $\mu\psi_0^R(\mu)$, which is equal to wt, the weight of the particle. We are relying on the linear nature of the (discretized) transport equation by only considering one element of the source at a time. With the source given, we solve for $\psi_1^L(\mu)$ and $\psi_1^R(\mu)$.

Suppose instead that we have an internal source. We first sample the cell in which the particle is born. We also sample the particle's direction and weight. Internal source particles may have weights different from unity due to source normalization, such as in the case of starting ten particles from three uniform cells with identical internal sources. Then, according to the particle's direction, we solve either Eq. (20) for $\mu > 0$ or Eq. (21) for $\mu < 0$. Again, every element of the source is zero except for $\frac{1}{2}q_i^L\Delta x_i$ and $\frac{1}{2}q_i^R\Delta x_i$, which we determine using the fact that, at this point, $wt = \frac{1}{2}q_i^A\Delta x_i$,

$$\frac{1}{2}q_i^L\Delta x_i = \frac{1}{2}q_i^A\Delta x_i\frac{q_i^L}{q_i^A} = wt\frac{q_i^L}{q_i^A} \quad , \tag{30}$$

$$\frac{1}{2}q_i^R\Delta x_i = \frac{1}{2}q_i^A\Delta x_i\frac{q_i^R}{q_i^A} = wt\frac{q_i^R}{q_i^A} \quad . \tag{31}$$

With the internal source given, we solve for $\psi_i^L(\mu)$ and $\psi_i^R(\mu)$.

4.2 Leakage or Collision

We have started a source particle—either an incoming flux particle or an internal source particle—and solved for the angular fluxes in the given cell. We then use the newly calculated angular fluxes to calculate the probabilities for leaking out of the cell and colliding in the cell—Eqs. (23) to (25) for $\mu > 0$ and Eqs. (27) to (29) for $\mu < 0$. If our sampling determines that the particle leaks out of the cell, it escapes the other side of the cell, maintaining its weight and direction, and serves as an incoming flux for the next cell. If the current cell is on the boundary of the system, the particle may either escape the system or reflect back into the cell. If the sampling dictates that the source particle collides in the cell, we must sample, based upon cross sections, whether the collision is an absorption or scatter. If the particle is absorbed, its life is over, and we start another source particle.

4.3 Isotropic Scattering

If we sample a scatter for the particle, we sample a new direction cosine, μ_s, from an isotropic distribution, and, setting μ=μ_s throughout, we solve either Eq. (20) for $\mu_s > 0$ or Eq. (21) for $\mu_s < 0$. Again, every source element is zero except for the scattering terms, $\frac{1}{2}\tau_{s,i}\phi_i^L$ and $\frac{1}{2}\tau_{s,i}\phi_i^R$. Since we have determined that the particle will scatter, the particle weight is equal to the scattering source: $wt = \frac{1}{2}\tau_{s,i}\phi_i^A$. The best estimate of the scalar flux is our most recent estimate of the angular flux, so

we determine the scattering source terms as follows:

$$\frac{1}{2}\tau_{s,i}\phi_i^L = \frac{1}{2}\tau_{s,i}\phi_i^A\frac{\phi_i^L}{\phi_i^A} = wt\frac{\psi_i^L}{\psi_i^A} \quad , \tag{32}$$

$$\frac{1}{2}\tau_{s,i}\phi_i^R = \frac{1}{2}\tau_{s,i}\phi_i^A\frac{\phi_i^R}{\phi_i^A} = wt\frac{\psi_i^R}{\psi_i^A} \quad . \tag{33}$$

So, we solve for new values of the left and right angular fluxes with the scattering source terms. The newly calculated angular fluxes and the scattering source terms are used to calculate probabilities of leaking out of the cell and colliding in the cell. If sampling deems that the particle leaks out of the cell, the particle escapes the cell out the side toward which it is pointing. The escaping particle maintains its weight and direction cosine and becomes an incoming flux particle to the next cell, escapes the system, or reflects back into the cell. If sampling deems the particle to collide, further sampling dictates whether the particle gets absorbed or scatters again. Thus, S_∞ converges the scattering source no faster than unaccelerated S_N or unbiased Monte Carlo.

5 Tallies

Tallies in the S_∞ method are essentially the same as in regular analog Monte Carlo particle transport. For instance, we can tally surface partial currents and surface scalar fluxes in the usual way [Lewis and Miller, 1984]. The left and right scalar fluxes are estimated by averaging the respective left and right angular fluxes from every discrete transport solve,

$$\phi_{i,total}^{L/R} = \frac{1}{N}\sum_n\sum_{k_n}\psi_{i,k_n}^{L/R}(\mu_{k_n}) \quad , \tag{34}$$

where N is the total number of particles, $n \in [1, N]$ is the particle index, and k_n is the event of particle n for which a discretized transport equation is solved, i.e., incoming flux, internal source, or scattering source. Estimates of the variance are done the usual way by accumulating the square of each particle's contribution in each cell [Lewis and Miller, 1984].

6 Correct S_∞ Scattering

There is an important subtlety in the S_∞ scattering. For certain situations involving high scattering and low leakage, negative angular fluxes are possible on the weak side of the cell—the side away from the particle direction. These negative angular fluxes may translate into negative leakage probabilities if the particle scatters back toward the side with a negative angular flux. We first discuss the correct, analog way to handle these negative probabilities. Then we derive an antithetic variates approach that avoids negative probabilities altogether. For the degenerate case of isotropic scattering in one-dimensional slab geometry, we call this antithetic variates approach "two-scatter variance reduction."

6.1 Handling Negative Probabilities

With two mutually exclusive probabilities, $P_{leak} + P_{collide} = 1$, we require that the total weight, wt, entering the sampling be conserved:

$$P_{leak}\ wt_{leak} + P_{collide}\ wt_{collide} = wt \quad , \tag{35}$$

where wt is the incoming weight, wt_{leak} is the weight of a leaking particle, $wt_{collide}$ is the weight of the particle after colliding, $P_{leak}wt_{leak}$ is the expected leakage weight, and $P_{collide}wt_{collide}$ is the expected colliding weight. If, as in the analog situation, the particle weight does not change, i.e., $wt_{leak} = wt_{collide} = wt$, then total weight is indeed conserved.

Now, when one of the probabilities is negative, we see that the total normalized probability, $|P_{leak}| + |P_{collide}|$, is not equal to unity. In order to sample in the realm (0,1), we must normalize the probabilities,

$$\tilde{P}_{leak} = \frac{|P_{leak}|}{|P_{leak}| + |P_{collide}|} \quad , \tag{36}$$

$$\tilde{P}_{collide} = \frac{|P_{collide}|}{|P_{leak}| + |P_{collide}|} \quad . \tag{37}$$

Requiring that these normalized probabilities conserve the analog expected leakage and colliding weight, we obtain, in the presence of negative probabilities, the weight of a particle after a leak and after a collision,

$$wt_{leak} = wt\frac{P_{leak}}{|P_{leak}|}\left(|P_{leak}| + |P_{collide}|\right) \quad , \tag{38}$$

$$wt_{collide} = wt\frac{P_{collide}}{|P_{collide}|}\left(|P_{leak}| + |P_{collide}|\right) \quad . \tag{39}$$

These equations say that, if either of the probabilities are negative, the particle weight must increase by a factor of $\left(|P_{leak}| + |P_{collide}|\right)$ regardless of which event is sampled. If the event with a negative probability is sampled, the sign of the weight must be switched. While this technique is unbiased, it is not entirely practical. In extreme cases of high scattering and low leakage, the particle weights increase to very large positive and negative values.

6.2 Two-Scatter Variance Reduction

Sometimes the best way to deal with a problem is to avoid it. The premise behind antithetic variates is that the average of two negatively correlated estimates has a lower variance [Carter and Cashwell, 1975]. With isotropic scattering, we can easily sample a direction cosine *and its negative* at the same time. Instead of averaging two estimates in a post-sample fashion, we average the probability equations for both directions and obtain a new probability equation that includes leakage out both sides of the cell. Practically speaking, this approach eliminates the weak side of the cell during a scatter and avoids negative probabilities altogether.

After sampling a scattered direction, μ_s, we solve Eq. (20) for $|\mu_s|$ and Eq. (21) for $-|\mu_s|$. Utilizing "+" superscripts for angular fluxes in the $|\mu_s|$ direction and "–" superscripts for angular fluxes in the $-|\mu_s|$ direction, we substitute the angular fluxes into the probability equations, Eqs. (22) to (25) and Eqs. (26) to (29). Noting that, in the scattering case, both Q_i^+ and Q_i^- are equal to $\frac{1}{2}\tau_{s,i}\phi_i^A$, we drop the superscripts on Q_i and average the two probability equations to obtain

$$\hat{P}^+_{leak} + \hat{P}^-_{leak} + \hat{P}_{collide} = 1 \quad , \tag{40}$$

where

$$\hat{P}^{+}_{leak} = \frac{|\mu_s|\psi_i^{+R}}{2Q_i} \quad , \tag{41}$$

$$\hat{P}^{-}_{leak} = \frac{-|\mu_s|\psi_i^{-L}}{2Q_i} \quad , \tag{42}$$

$$\hat{P}_{collide} = \frac{\tau_i\left(\psi_i^{+A}+\psi_i^{-A}\right)}{2Q_i} = \frac{\frac{1}{2}\tau_i\left(\psi_i^{+L}+\psi_i^{+R}+\psi_i^{-L}+\psi_i^{-R}\right)}{2Q_i} \quad . \tag{43}$$

This new probability equation includes probabilities for leakage out both sides of the cell and eliminates negative probabilities due to scattering. Since the directions $|\mu_s|$ and $-|\mu_s|$ are equally weighted, the new angular flux for each side of the cell is the average of the angular flux due to each direction.

7 Results

We compare our S_∞ results to both analytical and deterministic, LLD, S_{32} solutions. For the essential, but uninteresting cases of purely streaming and purely absorbing (both with normally incident flux), we merely report that S_∞ admits both analytic solutions: a delta function and an exponential. We present results for two problems: 1) an almost–normally incident flux on a purely scattering slab, and 2) a fixed source problem. Finally, we compare S_∞ with analog scattering to S_∞ with two-scatter variance reduction.

7.1 Purely Scattering Slab with Normally Incident Flux

We consider a 100–mfp purely scattering slab with an almost–normally incident flux. The direction cosine of the incoming flux is μ_{in}=0.99726386184982, the S_{32} discrete direction closest to normal. Figure 1 compares the S_{32} and S_∞ results. Meeting expected coverage rates, the S_∞ results are within one standard deviation of the S_{32} results for about 67% of the cell edges.

7.2 Fixed Source

Here, we consider a fixed source test problem proposed by Reed [Reed, 1971]. The problem tests a method's ability to deal with regions of greatly differing characteristics. For us, it specifically tests the internal source. Table 1 describes the physical characteristics of the slab.

Table 1: Physical description of the Reed test problem.

	$0 < x < 2$cm	$2 < x < 3$cm	$3 < x < 5$cm	$5 < x < 8$cm
σ_t	50.0	5.0	0.0	1.0
σ_s	0.0	0.0	0.0	0.9
q^A	50.0	0.0	1.0	0.0
Δx	0.2	0.2	0.2	0.2

Figure 2 compares S_∞ using 10^8 particles to the LLD, S_{32} solution. The solutions agree, with the inordinate number of particles producing very small error bars.

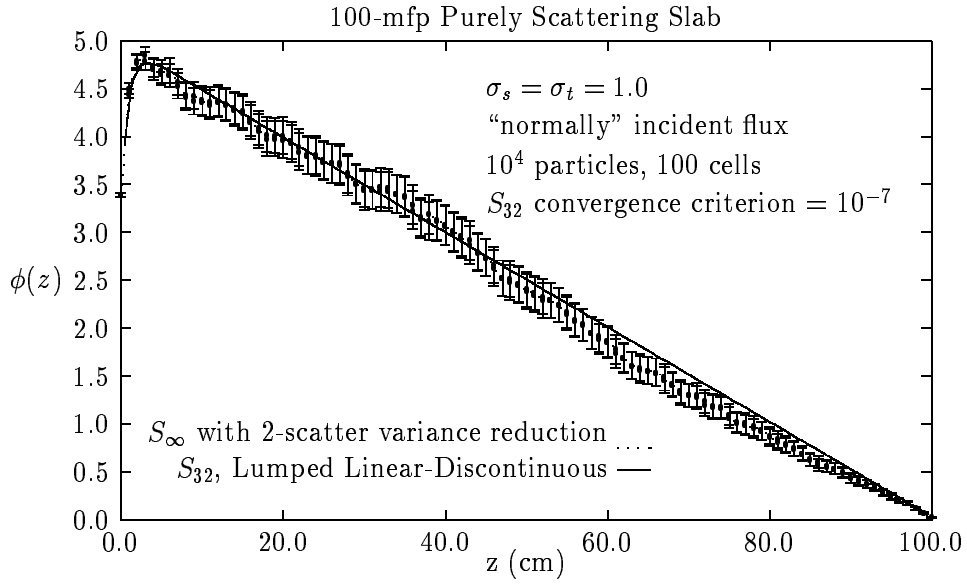

Figure 1: S_∞ with two-scatter variance reduction, plotted with one-standard-deviation error bars, and S_{32} for a purely scattering, 100-mfp thick slab.

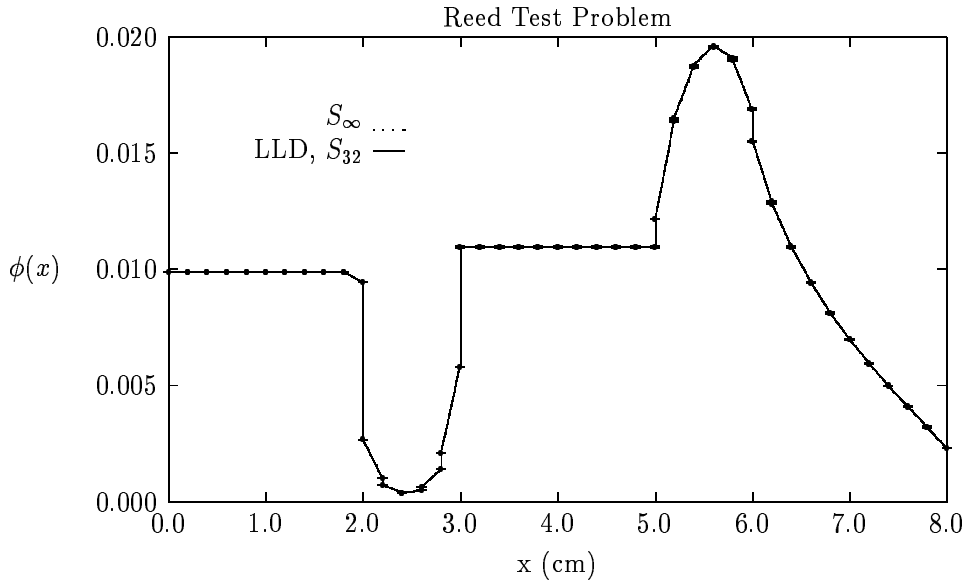

Figure 2: Fixed source test problem by Reed.

7.3 Two-Scatter Variance Reduction

We quantitatively examine the advantages of the two-scatter variance reduction over the unbiased, analog scattering in S_∞ by defining a calculation's quality as

$$Q = \frac{1}{t_{cpu}\ \max(\sigma^2)} \quad , \tag{44}$$

where t_{cpu} is the cpu time in seconds (on a TATUNG Super COMPstation 20) and $\max(\sigma^2)$ is the maximum variance in the cell-edge scalar fluxes. Using Q, we compare analog scattering to two-scatter variance reduction for purely scattering slabs of increasing thickness, as shown in Fig. 3. Two-scatter variance reduction is not as important in thin systems because particles will leak out before

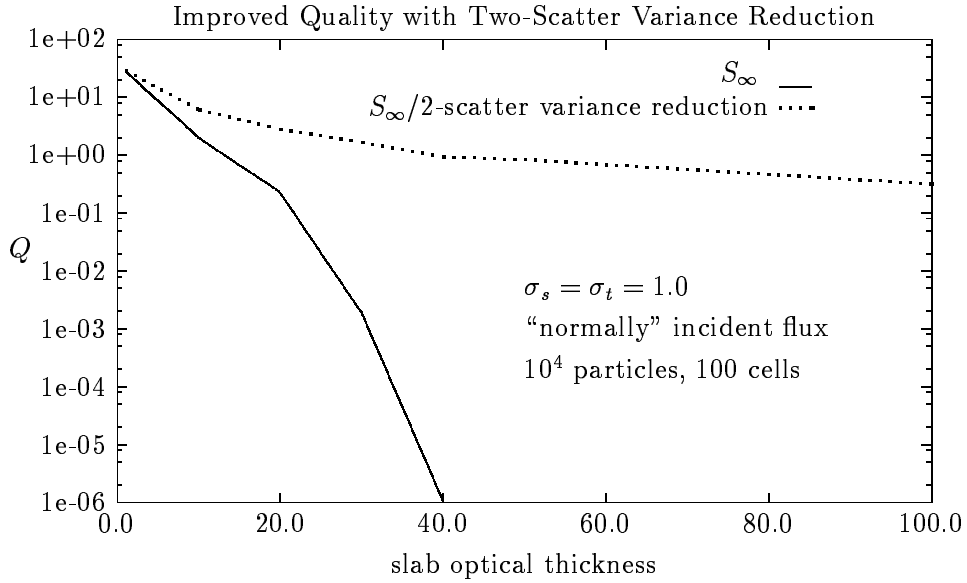

Figure 3: Quality values for S_∞ with and without two-scatter variance reduction.

they could possibly gain too much weight. The two-scatter variance reduction required about 5–10% more cpu time than analog scattering for slabs 10 to 50 mfps thick. For the 100–mfp slab, the two-scatter variance reduction calculation required 74 seconds, whereas the analog scattering calculation still had not finished after 10 hours.

In Figure 4, we demonstrate the quality by plotting the scalar fluxes for the two cases. The analog scat-

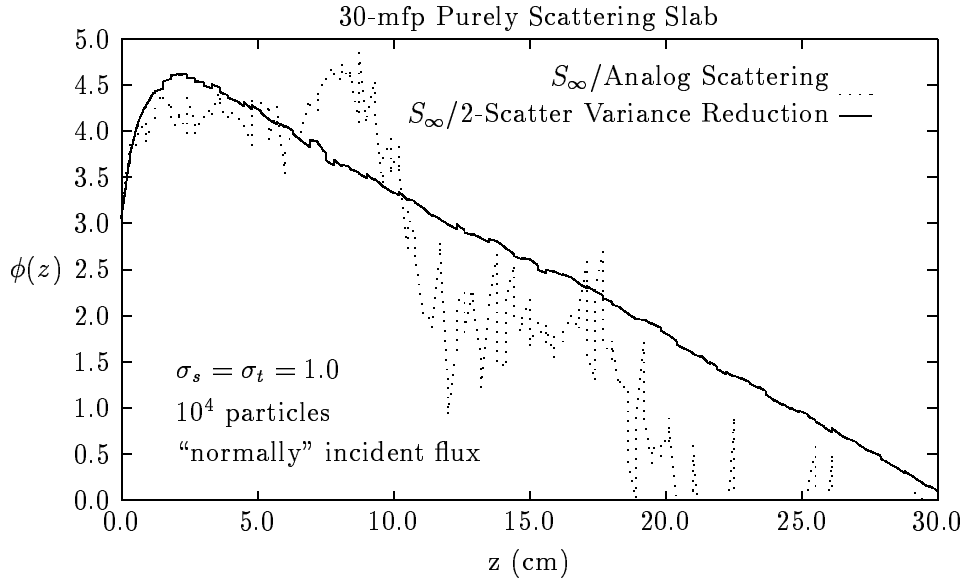

Figure 4: S_∞, with and without two-scatter variance reduction, on a 30-mfp purely scattering slab.

tering case had particle weights ranging from -764 to 389, whereas the weights in the two-scattering variance reduction case did not deviate from unity. The maximum standard deviations of the scalar flux were 3.68 for analog scattering and 0.118 for the two-scatter variance reduction.

8 Conclusions

We have presented a new hybrid method, the S_∞ method, for steady-state, mono-energetic neutron transport in one-dimensional slab geometry with isotropic scattering and an isotropic internal source. The S_∞ method considers Monte Carlo particles that are continuous in angle and that traverse discrete space. We have shown the viability of the method in one dimension by successfully comparing to analytic and deterministic results.

Acknowledgments

This work was performed under the auspices of the U.S. Department of Energy. We gratefully acknowledge Todd Palmer for his comments and his LLD code for the fixed source problem, Todd Wareing for test problem information, Tom Evans for computer assistance, and Pat Mendius for her editing.

References

[Fleck and Cummings, 1971] J. A. Fleck, Jr., and J. D. Cummings, An Implicit Monte Carlo Scheme for Calculating Time and Frequency Dependent Nonlinear Radiation Transport, Journal of Computational Physics, 8, pages 313-342 (1971).

[Morel, et al., 1996] J. E. Morel, Todd A. Wareing, and Kenneth Smith, A Linear-Discontinuous Spatial Differencing Scheme for S_n Radiative Transfer Calculations, Journal of Computational Physics, 128, pages 445-462 (1996).

[Urbatsch, et al., 1999] Todd J. Urbatsch, Jim E. Morel, and John C. Gulick, Monte Carlo Solution of a Spatially-Discrete Transport Equation, Part II: Diffusion and Transport/Diffusion, these proceedings (1999).

[Lewis and Miller, 1984] E. E. Lewis and W. F. Miller, Jr., Computational Methods of Neutron Transport, John Wiley & Sons, Inc., New York (1984).

[Carter and Cashwell, 1975] L. L. Carter and E. D. Cashwell, Particle-Transport Simulation with the Monte Carlo Method, TID-26607, ERDA Critical Review Series, Technical Information Center, U.S. Energy Research and Development Administration, Oak Ridge, TN (1975).

[Reed, 1971] W.H. Reed, New Difference Scheme for the Neutron Transport Equation, Nuclear Science and Engineering, 46, pages 309-314 (1971).